A storage model approach to the assessment of snow depth trends

Jonathan Woody,[1] Robert Lund,[1] Andrew J. Grundstein,[2] and Thomas L. Mote[2]

Received 18 March 2009; revised 9 July 2009; accepted 27 July 2009; published 20 October 2009.

[1] This paper introduces a stochastic storage model capable of assessing trends in daily snow depth series. The model allows for seasonal features, which permits the analysis of daily data. Breakpoint times, which occur when the observing station changes location or instrumentation, are shown to greatly influence estimated trend margins and are accounted for in this analysis. The model is fitted by numerically minimizing a sum of squares of daily prediction errors. Standard errors for the model parameters, useful in making trend inferences, are presented. The methods are illustrated in the analysis of a century of daily snow depth observations from Napoleon, North Dakota. The results here show that snow depths are significantly declining at Napoleon, with spring ablation occurring earlier, and that breakpoint features are very influential in deriving realistic trend estimates.

Citation: Woody, J., R. Lund, A. J. Grundstein, and T. L. Mote (2009), A storage model approach to the assessment of snow depth trends, *Water Resour. Res.*, *45*, W10426, doi:10.1029/2009WR007996.

1. Introduction

[2] This paper introduces a statistical method to assess long-term trends in snow depth time series. Snow is an important geophysical and environmental quantity that is very sensitive to climate change since its magnitude depends on both temperature and precipitation [*Kukla*, 1979; *Barry*, 1990]. Global climate models indicate that snow cover changes will considerably impact the cryospheric portion of the water budget in a greenhouse enhanced climate [*Barnett et al.*, 2005]. Studies suggest that the duration of snow cover may decrease by 40% in the Canadian Prairies and by 70% in the Great Plains [*Boer et al.*, 1992; *Brown et al.*, 1995]. Negative trends in snow have been observed across many areas in the western United States [*Mote et al.*, 2005; *Hamlet et al.*, 2005]. Such changes can dramatically impact local hydrology. An earlier spring ablation in some regions of North America has been linked to earlier maximum stream flow dates [*Barnett et al.*, 2005; *Burn*, 1994]. Reduced snow cover has been linked to a lengthened growing season at high latitudes [*Myeni et al.*, 1997], while changes in snow depths have been tied to soil temperature changes across the Great Plains [*Schmidt et al.*, 2001; *Grundstein et al.*, 2005].

[3] Ground based snow depths, which are commonly measured and often have long periods of record, are frequently used in hydrological and climatological studies as surrogates for snow mass and as measures of thermal insulation of the ground. Furthermore, the long period of record available at many stations makes these data very useful for climate change assessments.

[4] While issues of data quality [*Robinson*, 1993] and data scaling [*Blöschl*, 1999] have previously been addressed, snow data have not been critically evaluated with regard to breakpoints. A breakpoint occurs whenever there is a change in the location of the station, a change in the observer, or a change in the station instrumentation. Breakpoints profoundly affect geophysical data such as temperatures [*Lu and Lund*, 2007], but no study has quantitatively examined breakpoint effects on snow data. Because of the blowing and drifting nature of snow, accounting for station location changes is critical: an observation taken in a shaded area near a fence can be much deeper than one taken in the open. Fortunately, our data comes replete with metadata, a history of the conditions under which the data was observed.

[5] This paper attempts to accurately quantify trends in daily snow depth series in a statistical manner. We focus on one station, illuminating the features in the record that are influential in trend assessment. The model introduced is capable of describing daily observations. Modeling daily data is a challenge for several reasons. First, day-to-day snow depths are highly correlated in time and inference methods that assume independent and identically distributed data will give exaggerated levels of statistical confidence (*Fuller* [1996] is a comprehensive reference on such issues). Second, daily snow depths have a seasonal structure, with larger depths being more common in midwinter through early spring. Third, snow depths cannot be negative, but have a positive probability of being zero. In fact, snow depths are zero during the summer at all but the most alpine or Arctic stations. Accurate inferences should take into account this "zero modified support set issue." *Marsh* [1999] is a good general snow dynamic reference.

[6] The model we adopt is rooted in storage modeling. The only other author to pursue storage models in describing snow depths is *Perona et al.* [2007], who employs a model with two phases: increasing snow depths (the accumulation phase) and decreasing snow depths (the ablation phase). The model in the work of *Perona et al.* [2007] does

[1]Department of Mathematical Sciences, Clemson University, Clemson, South Carolina, USA.
[2]Department of Geography, University of Georgia, Athens, Georgia, USA.

0043-1397/09/2009WR007996$09.00

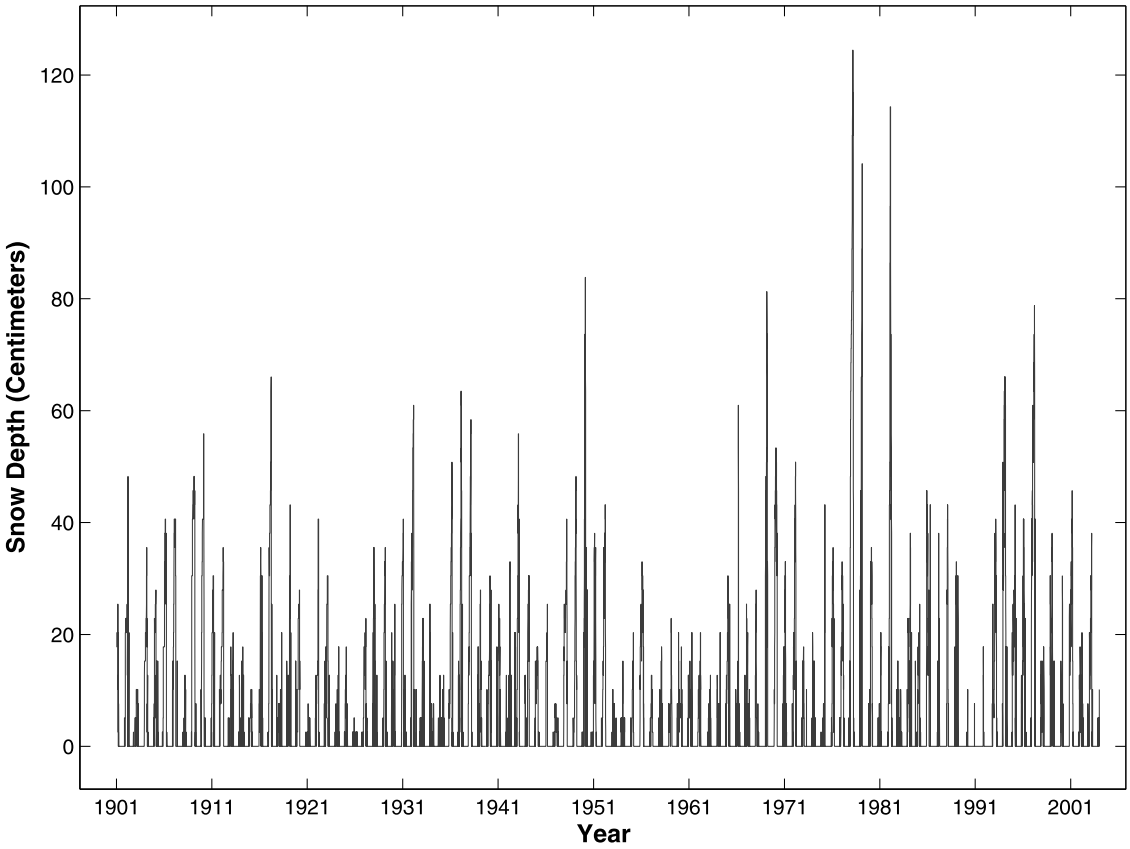

Figure 1. Daily snow depths at Napoleon, North Dakota, from 1 January 1901 to 6 December 2003.

not have a trend component nor does it allow for melting during the accumulation phase or accumulation during the ablation phase.

[7] The rest of this paper proceeds as follows. Section 2 introduces the data set that we study, a century of daily snow depth observations from Napoleon, North Dakota. Section 3 describes a storage model for the snow depth process; such a model allows for the features noted above. Section 4 shows how to estimate the parameters in the model, and section 5 applies the methods to make inferences about snow depth changes at Napoleon. Section 6 concludes with comments.

2. Napoleon Data

[8] Figure 1 displays 37595 daily snow depth observations taken at Napoleon, North Dakota from 1 January 1901 to 31 December 2003. Napoleon is located at latitude 46°30′17″N, longitude 99°46′1″W, resides at 1959 feet above sea level, has a mean annual temperature of 40.45 degrees F, receives 17.9 inches of liquid precipitation a year, and 36.4 inches of snow per year. This data has a well documented station history and extends back over 100 years. Only about 1.5% of the daily observations are missing, mostly at "seemingly random times." *Robinson* [1993] judged the Napoleon record to be of a uniquely high quality after performing intensive quality checks of stations across the United States. In Figure 1, one can see that peak snow depths vary considerably from year to year. The late 1970s are exceptionally snowy. A simple linear estimate of the annual snowfalls at Napoleon from 1931–2003 shows a positive increase of 0.633 cm per year. This increase in new snow may not translate to increasing snow depths for a variety of reasons, including increasing temperatures which may lead to snowpack compaction and ablation.

[9] To gain a feel for an annual snow depth cycle, Figure 2 shows the observations for the 1977–1978 winter season. For this snow season, depths peaked in early March, followed by spring ablation in early April. Snow from October and November storms is evident, but rapidly melted off. Snow cover was continual from early December until spring ablation in early April. These depths do not appear to compactify between snowfall events. It is unclear to us whether this is a consequence of the observing techniques, the climatological characteristics of the site, or the fact that the original depths were rounded to the nearest inch (or some combination thereof). As our model accommodates data of any type, this issue is not overly important in what follows.

[10] Table 1 shows the metadata record for the Napoleon station. Over the 103 years of record, there are some 18 changes in station location, observer, and observation times. Any of these changes may induce a level shift in the series. A casual inspection of Figure 1 and Table 1 reveals concerns. In particular, the three largest snow depths occurred during the 1976–1985 regime when the recording station is listed as Warren Wentz's Mother's house. Whether or not this era was truly this snowy is confounded with breakpoint and station location issues. Because of drifting tendencies, snow depths can significantly vary when the measuring location is moved only a few feet. While reference station comparisons could partly resolve such

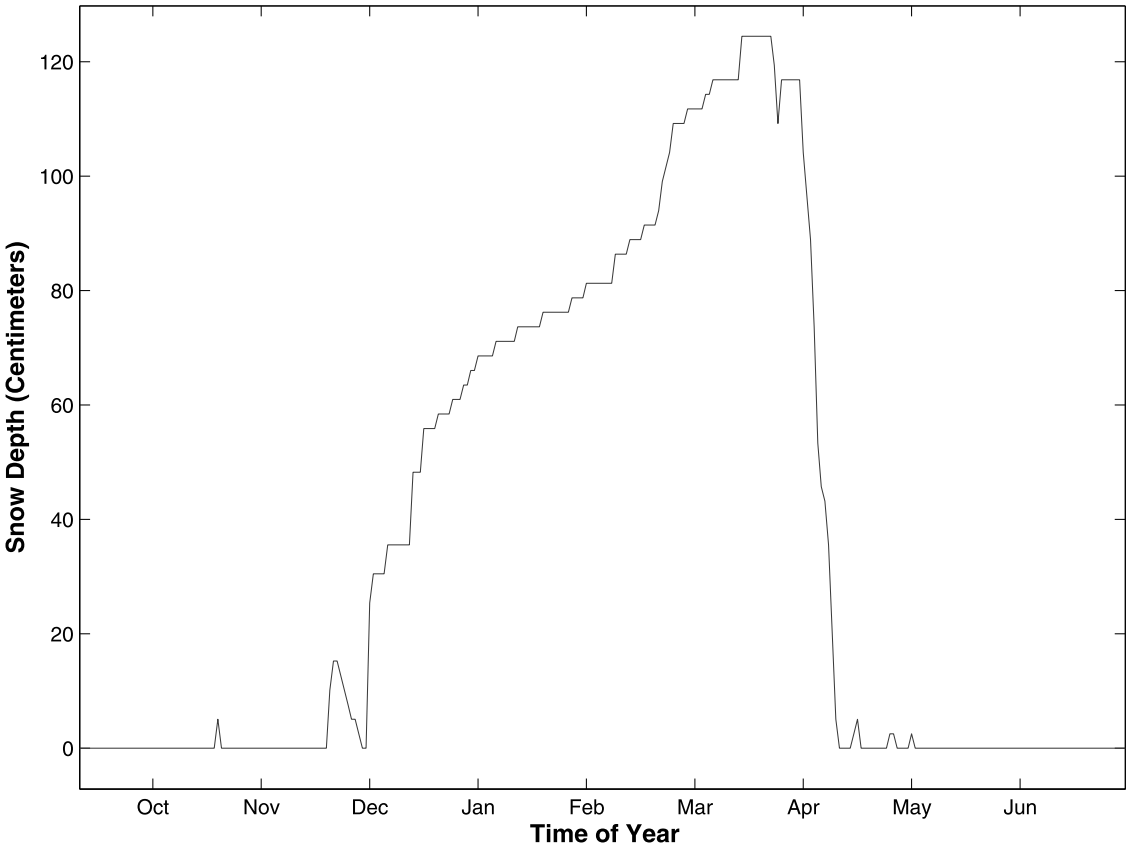

Figure 2. Daily Napoleon snow depths during the winter of 1977–1978.

issues, no good reference station exists that spans the duration of the record. The point here is that single station methods will need to take into account breakpoint information in examining long-term trends in the snow depth record. With the problem and data now elaborated upon, we introduce a model capable of assessing trends.

3. A Discrete Time Periodic Storage Model

[11] This section introduces our model of the snow depth process. Let X_t denote the snow depth at time t. Because the amount of snow on the ground is a stored quantity, we adopt a storage type model. Our model is based on the storage balance equation

$$X_t = \max\{X_{t-1} + Z_t, 0\}, \tag{1}$$

where Z_t is a random variable quantifying statistical changes in the pack occurring from time $t-1$ to t. View Z_t as the net change of snow (new minus meltoff) should the snow pack at time $t-1$ be so deep as to preclude ablation by day t. Because the data are observed daily (and not continuously) and snow depths cannot be negative, the maximum in (1) serves to prevent the pack content from becoming negative. We assume that $\{Z_t\}$ is white noise, independent of $\{X_t\}$, with periodic dynamics: $E[Z_t] = m_t$ and $\mathrm{Var}(Z_t) = w_t^2$. Periodic dynamics allow depth increases to be more likely in winter seasons. For convenience, we assume that Z_t is normally distributed. As the inferential objective here lies with trends, which are changes in the first moment, the normal assumption is not overly crucial. Should one be interested in extremes of the snow depths, then a marginal distribution with heavier tails could be used for $\{Z_t\}$.

[12] For seasonal dynamics, we assume that $\{m_t\}$ and $\{w_t\}$ are periodic in time with period $T = 365$ days. Using a first-order Fourier expansion to describe the seasonal mean component, we write

$$m_t = P_t\left\{A + B\cos\left(\frac{2\pi(t-\rho)}{T}\right) + \delta_t + \alpha t\right\}, \tag{2}$$

where ρ denotes the expected time of maximal daily increase of the pack and A and B are the mean and amplitude, respectively, of the sinusoidal expansion. The quantity α is the slope in a linear trend component and is the focal point of our future inferences. In (2), P_t is a deterministic indicator that is unity at times of the year when snowfall is possible and zero otherwise. This quantity stabilizes the ensuing numerical optimizations; specifically, it keeps the model optimization step and search routine from examining candidate models where large snow depths are possible during the summer. The quantity δ_t accounts for the breakpoints in the series; we assume the step form

$$\delta_t = \begin{cases} \Delta_1, & 1 \le t < \eta_1 \\ \Delta_2, & \eta_1 \le t < \eta_2 \\ \vdots & \vdots \\ \Delta_k, & \eta_{k-1} \le t \le N \end{cases},$$

where $\eta_1 < \eta_2 < \ldots < \eta_{k-1} \le N$ denote the ordered breakpoint times in the metadata. Perusing the metadata in

Table 1. Napoleon Metadata

Date	Station	Time	Change	Observer	Note
19 Aug 1939		1800	Site was already established	C. J. Hoof	Station began 1 Apr 1889 1.3 mi SE of PO
20 Jun 1946		0745	New observer, no move	G. Peterson	Station 1.5 mi SE of post office
8 Jul 1948			Station moved to another part of farm	G. Peterson	New thermometer support
11 Nov 1949		1830	Moved 70 feet SE to improve exposure	G. Peterson	1.3 mi SE of post office
17 Mar 1954	1	1800	Moved to 1.5 mi NW of Napoleon	T. Frank	0.3 mi N of post office
18 Apr 1956	1A		New observer, no move	A. Schuchard	
19 Feb 1957	1B		New observer, no move	W. Wentz	
8 May 1957	2	1800	New observer, moved	G. Peterson	At ice cream store 3 blocks east of PO, 3.5 blocks SE of old location
1 Jul 1958	2A		Recording rain gauge removed		
28 Aug 1958	3	1800	Equipment moved 0.6 mi W to observer's house	G. Peterson	Moved to 0.3 mi W of PO
30 Sep 1965	4	1800	No move, update form	G. Peterson	
10 Sep 1968	4A		New observer, no move	W. Wentz	
18 Aug 1969	5	0700	Moved to Soo Depot, 0.5 mi E	W. Wentz	Moved to more convenient location, station at 0.1 mi NE of PO
1 Dec 1973	5A		New observer, no move	T. Wentz	No move
14 Jun 1976	6	0700	Moved to mother's house 0.4 mi NE	W. Wentz	Station at 0.5 mi NE
	6A		Address correction		
11 Jul 1985	6B	0700	Moved across street to observer's house	W. Wentz	MMTS installed
23 Dec 1987	7	0700	No move, update form		
20 Oct 1992	8	0800	Moved 0.1 mi SW to new residence	B. Wentz	Son of previous observer, now 0.4 mi NE of PO

Table 1, we consider 18 breakpoint times with η_1 = 8/19/1939, η_2 = 6/20/1946,..., η_{18} = 10/20/1992. While undocumented breakpoint times (changepoints) may exist, changepoint methods are beyond the scope of this paper. The form of δ_t is a step function which depends on the regime at which the data was recorded. We take $\Delta_1 = 0$ to keep all model parameters identifiable (else, take $A = 0$ as a baseline). The interpretation is that regime ℓ is more snowy than regime $\ell - 1$ (assuming a zero trend) when $\Delta_\ell > \Delta_{\ell-1}$.

[13] The model is easily modified to permit a seasonal trend component. For this, (2) is changed to

$$m_t = P_t\left\{A + B\cos\left(\frac{2\pi(t-\rho)}{T}\right) + \delta_t + \left[C + D\cos\left(\frac{2\pi(t-\xi)}{T}\right)\right]t\right\}. \quad (3)$$

In (3), C is the average trend and D and ξ are the amplitude and phase parameters of the seasonal trend deviations about C.

[14] Given these dynamics, $\{X_t\}$ is a discrete-time Markov chain on the state space $[0, \infty]$ with periodic transition probabilities. In continuous time, one can regard the process as a periodic diffusion with a boundary at state zero (diffusions are discussed by *Cox and Miller* [1965]). The data can be viewed as observations of such a continuous time process taken on a discrete time lattice. Such notions are not overly important: we will simply need to be able to compute predictions of the next snow depth measurement from past observations. We comment that the same storage model may prove useful in describing streamflow series with periodic features that run dry. Here, precipitation is regarded as input into the store and stream discharge is regarded as the output.

[15] It is tempting to try to develop more elaborate models for the snow depth process, for instance one in which Z_t is decomposed into a daily new snow accumulation minus a daily meltoff. However, as we will need to fit the model by conditional moment methods (this is discussed in the next section), parameter identifiability issues in such a decomposition would arise. Because of this, we do not pursue models that have separate components for new snow accumulations and meltoff.

4. Model Estimation

[16] This section discusses parameter estimation in the model. While likelihood estimators generally have the most favorable sampling properties, the likelihood function of the model is essentially intractable (this is known from queueing theory [*Basawa and Rao*, 1980]) and alternative approaches need to be considered. We will adopt a conditional moment approach based on quasi-likelihood and estimating equations. For clarity of exposition, we assume there is no missing data and ignore leap year effects.

[17] Let $\boldsymbol{\theta} = (A, B, \rho, \alpha, \Delta_2, \ldots, \Delta_k)'$ be a vector containing all model parameters (add C, D, and ξ to this vector should a seasonal trend be considered). A simple sum of squares based on one-step-ahead prediction errors is $\Sigma_{t=1}^{N} (X_t - \hat{X}_t)^2$, where $\hat{X}_t = E[X_t|X_{t-1}, \ldots, X_1]$. Here, $E[\cdot]$ denotes expectation and $E[X|Y]$ indicates the conditional expectation of X given Y. Since $\{X_t\}$ is a periodic Markov chain, $\hat{X}_t = E[X_t|X_{t-1}]$. Because the snow depth process has periodic characteristics, it is preferable to use weighted least squares techniques in lieu of ordinary least squares. This entails scaling the prediction errors during each season by an estimate of its variability. In particular, the sum of squares function that we will minimize is

$$S(\boldsymbol{\theta}) = \sum_{t=1}^{N} \frac{(X_t - \hat{X}_t)^2}{\sigma_t^2} = \sum_{n=0}^{d-1}\sum_{\nu=1}^{T} \frac{(X_{nT+\nu} - \hat{X}_{nT+\nu})^2}{\sigma_\nu^2}, \quad (4)$$

where $\sigma_t^2 = E[(X_t - \hat{X}_t)^2|X_{t-1}]$ and $d = N/T = 103$ is the number of years of data.

[18] It is not important to be precise with the seasonal weights σ_ν^2. In fact, optimizing a version of $S(\boldsymbol{\theta})$ without any seasonal weights gives asymptotically consistent estimators of all nonbreakpoint parameters; however, these estimators will not have a minimal variance (*Fuller* [1996, chapter 9] is

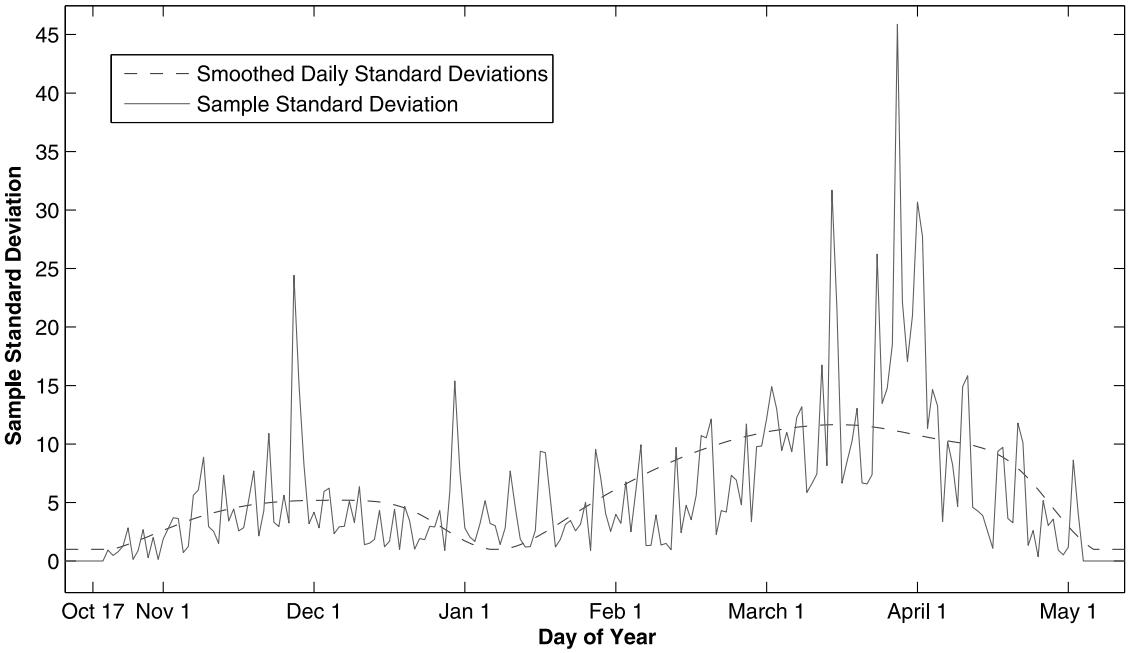

Figure 3. Estimated values of σ_ν^2. The dashed curve shows smoothed values estimated from a two-piece cosine fit.

a good reference discussing such issues). Here, we will use the simple sample variance weight

$$\sigma_\nu^2 = \frac{1}{d-1}\sum_{n=0}^{d-1}\left(X_{nT+\nu} - X_{nT+\nu-1}\right)^2. \tag{5}$$

This is because the conditional variance $\mathrm{Var}(X_{nT+\nu} - \hat{X}_{nT+\nu}|X_{nT+\nu-1})$ is the optimal choice of σ_ν^2 and away from the state space boundary at zero (bare ground) and

$$X_{nT+\nu} - \hat{X}_{nT+\nu} \approx X_{nT+\nu} - X_{nT+\nu-1} - Z_{nT+\nu}.$$

Phrased another way, $w_\nu \approx \sigma_\nu$.

[19] Figure 3 plots such empirical values of σ_ν^2 over all seasons ν. Also shown is a curve that smooths the empirical values; the smoothed versions were developed by fitting sinusoids to the spring and fall components and will be used in subsequent computations. Separate sinusoids were used before and after 1 January. This is because snow depth changes are the most variable during early spring when a full winter's pack has accumulated; depth changes during the height of winter appear to be less variable at Napoleon (likely due to consistent subfreezing midwinter temperatures). To aid numerical stability, we do not allow a weight to be less than unity. If a weight is very small, this season will contribute heavily to the sum of squares.

[20] An explicit form is needed for the conditional mean in (1). Appendix A derives

$$E[X_{t+1}|X_t] = \{X_t + m_{t+1}\}\left\{1 - \Phi\left(\frac{-X_t - m_{t+1}}{w_{t+1}}\right)\right\} + w_{t+1}\phi\left(\frac{X_t + m_{t+1}}{w_{t+1}}\right), \tag{6}$$

where $\Phi(x) = Pr[Z \le x]$ is the cumulative distribution function of the standard normal random variable and $\phi(x) = \Phi'(x)$ is the standard normal density function.

[21] Estimates of the parameters in $\boldsymbol{\theta}$ are found by numerically minimizing $S(\boldsymbol{\theta})$. Because of the seasonal weights and other nonlinearities of the objective function in the model parameters, this is necessarily a numerical task. Standard MATLAB packages have capably handled our problem. We use $w_\nu = \sigma_\nu$ in (6). One can consider strategies where w_ν is jointly optimized with m_ν, but this does not appear to be needed here.

[22] Inferences can be made by invoking asymptotic normality principles for estimators derived from sum of squares criterion [see *Klimko and Nelson*, 1978]. In particular, under appropriate sampling schemes, it can be shown that the estimator $\boldsymbol{\theta}$ that minimizes $S(\boldsymbol{\theta})$ is consistent and asymptotically normal in that the distributional convergence

$$\hat{\boldsymbol{\theta}} \xrightarrow{\mathcal{D}} N(\boldsymbol{\theta}, F/d),$$

as $d \to \infty$ is achieved. Here, F is a positive definite covariance (information) matrix and N represents a normal distribution. Following the classical arguments of *Klimko and Nelson* [1978], F/d can be approximated by the inverse of the second derivative matrix of $S(\boldsymbol{\theta})$ evaluated at $\boldsymbol{\theta} = \hat{\boldsymbol{\theta}}$:

$$F/d \approx \left[\frac{\partial^2 S(\boldsymbol{\theta})}{\partial\boldsymbol{\theta}\partial\boldsymbol{\theta}'}\right]^{-1}\Bigg|_{\boldsymbol{\theta}=\hat{\boldsymbol{\theta}}}. \tag{7}$$

This relation allows standard errors for the model parameter estimates to be obtained; these standard errors are simply the square roots of the diagonal components of F/d. Such standard errors enable us to tune the model fit, eliminating any breakpoint mean shift parameters that do not induce

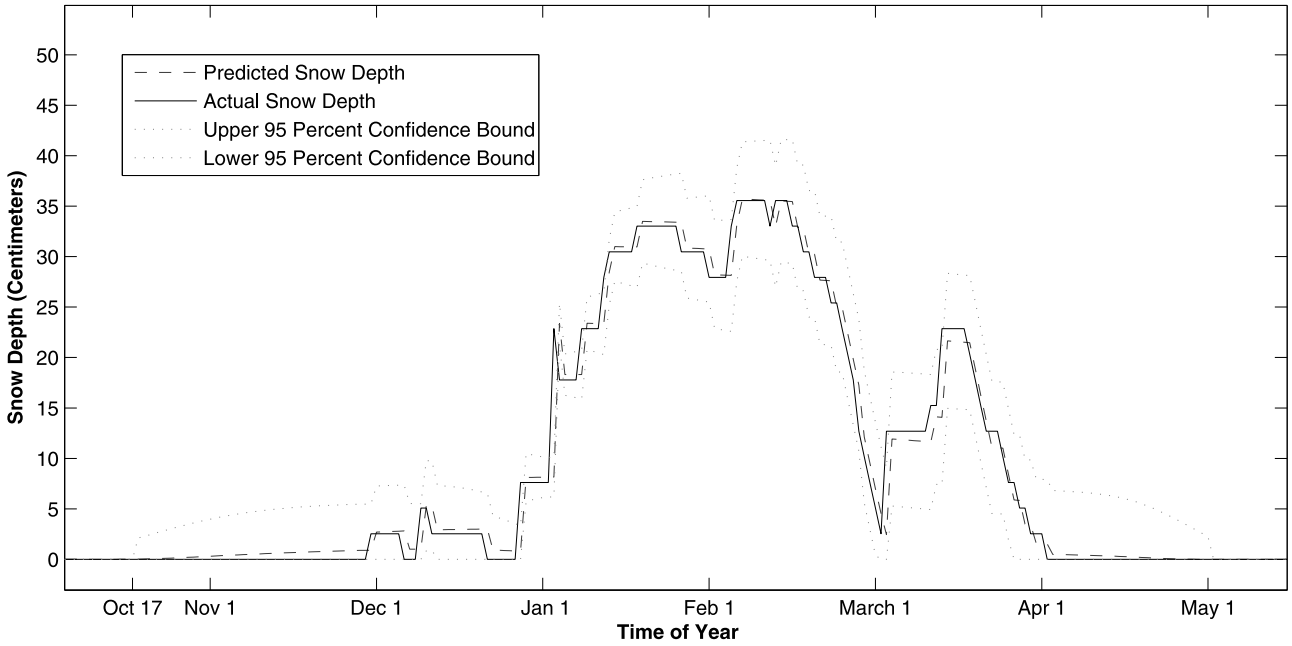

Figure 4. Snow depths with 1-day-ahead predictions (dashed). The 95% confidence bands are included.

significant changes. Eliminating insignificant model parameters allows one to improve accuracy margins of the trend estimator.

[23] Two caveats need to be added to the above stated asymptotic normality. First, a proof of asymptotic normality needs all snow processes to continue infinitely far into the future. When $\alpha < 0$, there will be a last time where it snows and snow processes eventually cease. Of course, α will be small in most practical situations and the last time where it snows may occur so far into the future as to render the sampling distribution of $\hat{\alpha}$ close to Gaussian. Second, the sampling scheme needed to easily prove asymptotic normality assumes that the number of data points sampled in each regime (in between all breakpoint times) converges to infinity as $d \to \infty$. Such infill asymptotics seem unrealistic here; in fact, it seems more plausible that the station location will move infinitely often over an infinite time horizon. An implication of the latter sampling scheme is that the mean shift sizes $\Delta_2, \ldots, \Delta_k$ cannot be consistently estimated. This said, it is expected, akin to *Lu and Lund* [2007], that asymptotic normality of $\hat{\alpha}$ could still be proven as long as the station does not move too often. The mathematics to such arguments is intense and will not be dealt with here. The next section presents a simulation showing that the sampling distribution of the trend estimator is very close to Gaussian for our situation (approximately a century of data with five significant breakpoints). We also point out that asymptotic normality is a limiting property that is routinely applied to finite samples of reasonable size; it should provide reasonable guidance here.

5. Results

[24] This section fits our storage model to the Napoleon data. We make two comments before proceeding. First, leap year effects will be ignored; in fact, the Napoleon data record lists 365 days for each and every year in the study (we are not sure how leap year effects were accounted for). Regardless, leap year effects should not change results appreciably. Second, a snow season is taken to run from 17 October to 1 May, so $P(t)$ is zero for times t sampled between 2 May and 16 October. No appreciable snow was observed outside of these days. Third, missing data must be dealt with. This issue is minimal with the Napoleon data as only about 1.5% of the record is missing during the snow season. If the datum point is missing at time t, we simply omit the terms from the summation in (4) at times t and $t + 1$ (omitting the time $t + 1$ observation is necessary since $\hat{X}_{t+1}$ also depends on X_t). Since most of the missing observations are not isolated, but rather occur in longer strings of weeks or months (often in summer months when $P(t)$ is zero), the total percentage of snow-season times missing from (4) is less than 3%.

[25] Figure 4 shows how the model fits the snow depths during the winter season of 1975–1976. This graphic displays the snow depth values against their predictions; 95% confidence bands are included and are derived from (1) and normal $\{Z_t\}$. Indeed, the predictions appear to be tracking the data reasonably well. However, the model does not resolve individual days in that the estimated snowpack is too small on days when it snows heavily. The estimates "catch back up" with the snow depths on the first day thereafter on which heavy snow does not fall.

[26] When all breakpoint times are ignored, the fitted trend estimate and one standard error is $\hat{\alpha} = 0.2250 \pm 0.0466$ cm per century. Because breakpoints induce mean uncertainties, their presence (or lack thereof) greatly impacts the estimated trend (*Lu and Lund* [2007] encounter the same issue in estimating temperature trends).

[27] Our next goal is to investigate the effects of breakpoints on the trend estimate. Of the 18 breakpoint times listed in Table 1, two occur during the summer of 1958. Because snow depths are zero during summer, both of these breakpoints cannot be "identified" with our data and we proceed with 17 total breakpoints, one during the summer of 1958. Such a duplication issue occurs only once. With all 17

Table 2. Summary of Model Parameter Estimates

Parameters	Seventeen Breakpoints	Five Breakpoints	No Breakpoints
A	−2.5982 (0.0755)	−2.5951 (0.0742)	−2.7224 (0.0678)
B	2.9144 (0.0707)	2.9062 (0.0700)	2.9002 (0.0700)
ρ	3.8374 (0.6811)	3.7964 (0.6823)	3.8986 (0.6810)
α	−0.5004 (0.1927)	−0.4748 (0.1803)	0.2250 (0.0466)
Δ_1 (19 Aug 1939)	0.2558 (0.0728)	0.2263 (0.0629)	-
Δ_2 (20 Jun 1946)	0.1269 (0.1114)	-	-
Δ_3 (8 Jul 1948)	0.4639 (0.1421)	-	-
Δ_4 (11 Nov 1949)	0.2419 (0.0911)	-	-
Δ_5 (17 Mar 1954)	0.1924 (0.1196)	-	-
Δ_6 (18 Apr 1956)	−0.0360 (0.1949)	0.0074 (0.0960)	-
Δ_7 (19 Feb 1957)	0.3707 (0.5387)	-	-
Δ_8 (8 May 1957)	−0.2248 (0.1905)	-	-
Δ_9 (1 Jul 1958)	-	-	-
Δ_{10} (28 Aug 1958)	0.0626 (0.0990)	-	-
Δ_{11} (30 Sep 1965)	−0.0381 (0.1327)	-	-
Δ_{12} (10 Sep 1968)	0.5633 (0.2352)	0.5626 (0.1118)	-
Δ_{13} (18 Aug 1969)	0.4975 (0.1225)	-	-
Δ_{14} (1 Dec 1973)	0.7380 (0.1559)	-	-
Δ_{15} (14 Jun 1976)	0.5899 (0.1285)	-	-
Δ_{16} (11 Jul 1985)	0.2021 (0.1685)	0.2835 (0.1442)	-
Δ_{17} (23 Dec 1987)	0.3923 (0.1685)	-	-
Δ_{18} (20 Oct 1992)	0.6332 (0.1565)	0.6123 (0.1473)	-

breakpoints in the model, the trend estimate and one standard error become $\hat{\alpha} = -0.5004 \pm 0.1927$ cm per century. Observe that the trend is now significantly negative.

[28] Many of the breakpoint times may not be accompanied with significant mean shifts; hence, our next task is to eliminate all insignificant breakpoint times in the metadata and recompute the trend estimate with only the significant breakpoints included. Such a procedure enables the trend and other model parameters to be more accurately estimated. The 17 remaining breakpoint times were subjected to a backward regression elimination procedure at level 95% [see *Anderson et al.*, 1994]. The magnitude of the level shift from regime i to regime $i + 1$ is $\Delta_{i+1} - \Delta_i$. The standard error for its estimated difference is hence

$$\mathrm{Var}(\hat{\Delta}_{i+1} - \hat{\Delta}_i) = \mathrm{Var}(\hat{\Delta}_{i+1}) + \mathrm{Var}(\hat{\Delta}_i) - 2\mathrm{Cov}(\hat{\Delta}_{i+1}, \hat{\Delta}_i), \tag{8}$$

which is easily estimated from components of the second derivative matrix F/d. We then compute the Z score

$$z_i = \frac{\hat{\Delta}_{i+1} - \hat{\Delta}_i}{\mathrm{Var}(\hat{\Delta}_{i+1} - \hat{\Delta}_i)^{1/2}}$$

for each breakpoint time i. At each iteration of the backward regression, the breakpoint with the smallest $|z_i|$ is eliminated as long as $|z_i|$ is smaller than the 95th standard normal percentile (two-sided) of 1.96. If all $|z_i|$ exceed 1.96, the elimination procedure is stopped. After each eliminated breakpoint, the model is refitted and the parameter estimates and standard errors are recomputed. In the end, five significant breakpoint times are retained. We do not see any significant patterns in the type of retained breakpoint (two are observer changes, two are station relocations, etc.). The trend estimate becomes -0.4748 ± 0.1803 cm per century. Notice that the standard error has decreased slightly from that for 17 breakpoints. The results of the backward elimination procedure are summarized in Table 2. Table 2 shows estimates of the model parameters when (1) all breakpoints are ignored, (2) all 17 of the breakpoint times are included, and (3) when the five significant mean shifts are accounted for. The times of the breakpoints were extracted from Table 1 and are noted in Table 2.

[29] At the 95% confidence level, the trend estimate when all 17 breakpoints is concluded to be negative. In fact, a two-sided p value of 0.0086 is obtained for the hypothesis test that snow depths are not changing. Hence, controlling for breakpoints, snow depths appear to be decreasing at Napoleon. The nontrend parameters all test as being significantly nonzero; hence, the model cannot be reduced further.

[30] Figure 5 graphically portrays the structure of the fitted models by plotting estimates of m_t against time t for no breakpoints, all 17 breakpoints, and only the five significant breakpoints. It is instructive to compare Figure 5 (middle and bottom) as it depicts which regimes have been eliminated. For instance, mean shifts for the very short regime in the late 1960s were deemed insignificant from the model fits and this regime was assimilated into a larger regime. The fitted model assigned the very snowy period during the late 1970s as part of a longer regime that had a significant upward mean shift.

[31] Since inferences were based on asymptotic normality, a simulation was run to check asymptotic normality of the sampling distributions. For this, 1000 replicates of the fitted time series were generated. In each simulation run, 103 years of the daily snow depth process were generated. Each simulation run has the five breakpoint times shown in the third column of Table 2. The magnitude of the mean shift at each breakpoint time and simulation run was randomly generated from a uniform distribution taking values over $[-1, 1]$. The other parameters in (2) were taken as those fitted to the Napoleon series, except that the trend α was taken as zero in all replications. Figure 6 shows a kernel density smoothed histogram of the 1000 estimates of α (one from each simulation run). Observe that these estimates

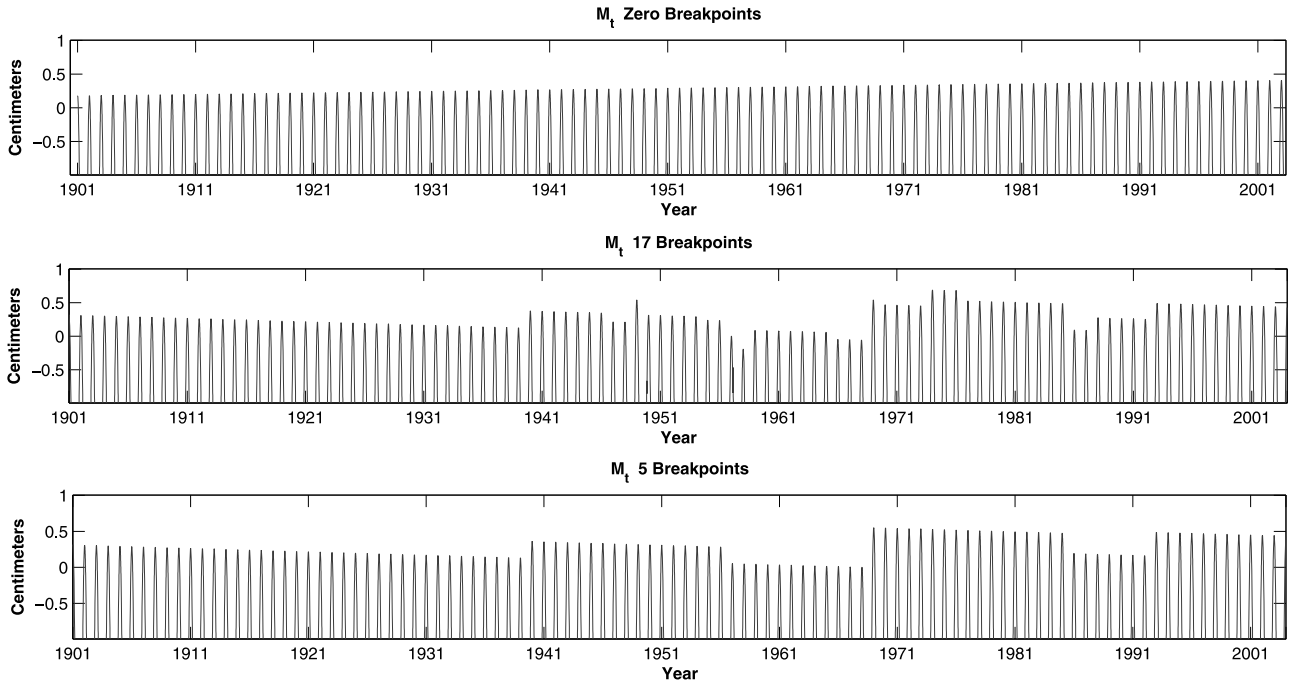

Figure 5. Structural form of m_t. Figure 5 depicts which breakpoints are retained in the backward elimination.

center around the true trend of zero and that their frequency distribution is unimodal and approximately normal. Hence, Gaussianity appears quite plausible for our sample sizes.

[32] Next, the model with the periodic trend in (3) was fitted allowing for the five significant breakpoints identified above; an estimate and one standard error of the seasonal trend parameter D is $\hat{D} = -0.6121 \pm 0.2400$ cm per century, suggesting with a p value of 0.0108 that trends are nonseasonal. The other parameter estimates in the model are $\hat{A} = -2.8687 \pm 0.1345$, $\hat{B} = 3.2190 \pm 0.1673$, $\hat{\rho} = 3.5016 \pm 1.0762$, $C = 0.0329 \pm 0.2844$, and $\hat{\xi} = -0.0761 \pm 9.6588$. The five mean shift estimates do not change appreciably from those listed in Table 2.

[33] To check on the seasonal fit, Figure 6 displays linear trend estimates for the depth observations for each day of year; for example, the 1 January trend is simply the trend slope, scaled to units of cm per century, of the 103 observations taken on 1 January. These daily trend estimates, computed via equation (3) in the work of *Lu and Lund* [2007], account for the five significant breakpoint times. The cosine wave fitted for the seasonal trend is superimposed on the graphic in Figure 7 and matches the rough structure of the daily trend estimates. Specifically, mid to late winter snow depths are decreasing most rapidly (ablation appears to be occurring earlier) and spring snow depths are showing a slight increase. It is also noted that a single cosine wave does not seem to describe the seasonal trends well. Higher-order Fourier fits, wavelet based expansions, or hinge-type structures such as those in the work of Livezey et al. (2007) could be explored.

[34] Before concluding, it is instructive to compare our methods to a naive trend analysis with seasonal snow tallies.

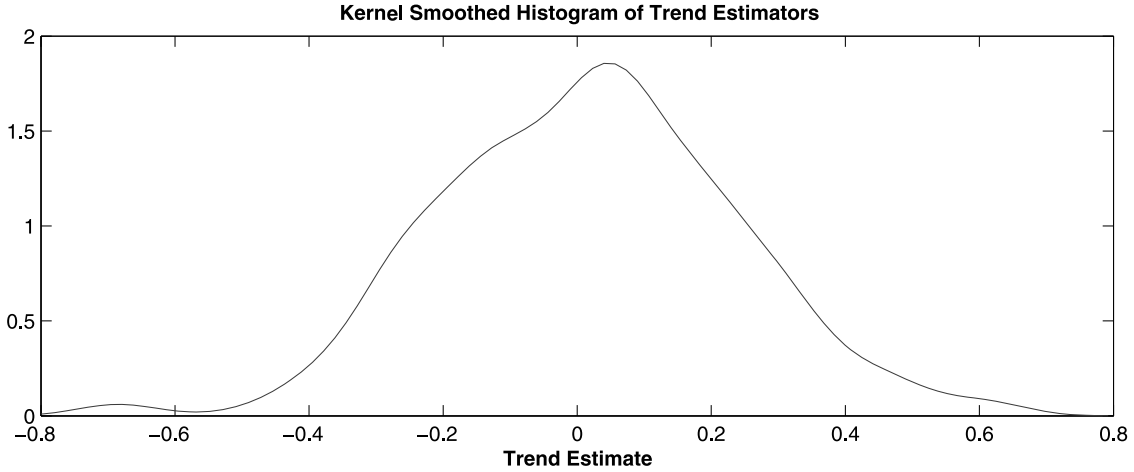

Figure 6. Kernel smoothed histogram of estimated trends showing approximately normality.

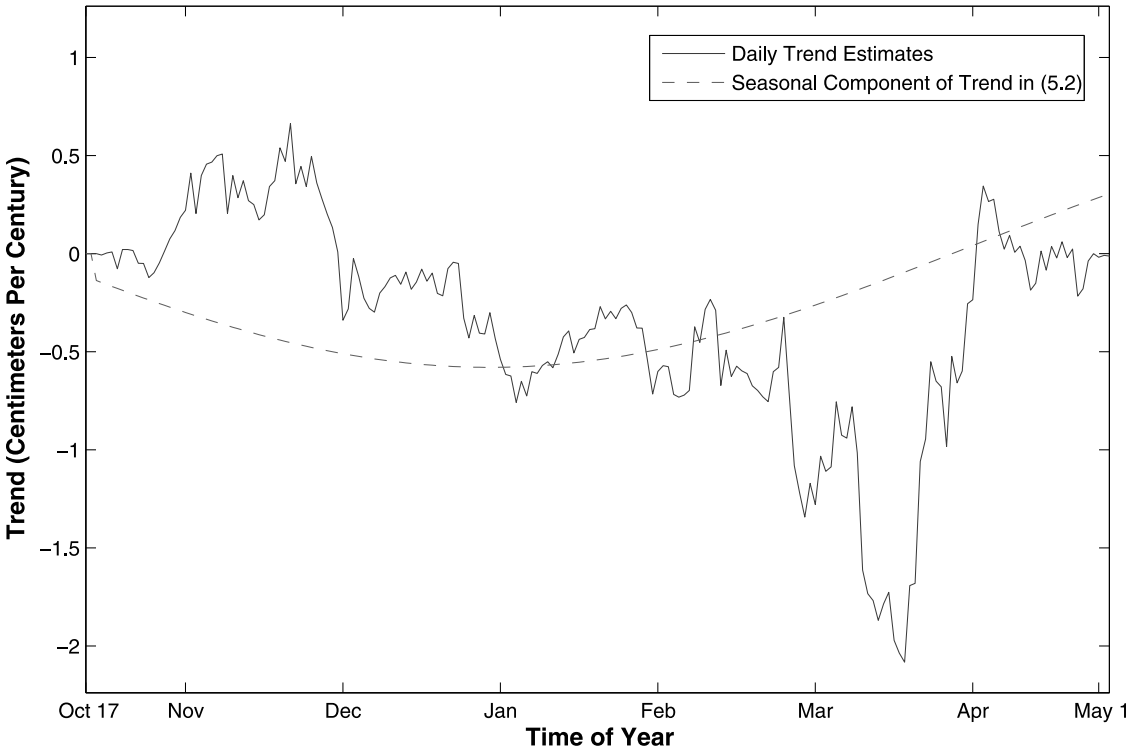

Figure 7. Daily trend estimates with superimposed Fourier fit.

Specifically, yearly snow totals were computed by adding the snow depth observations over all days during each snow season. As some seasons have too many missing data points to be considered reliable, seasons where more than 10% of the observations are missing were discarded in this comparison (i.e., are deemed as missing). Also, the 1901 spring and 2003 fall records were discarded since a complete record is not available for these winter seasons. In years where 10% or less of the snow season observations are missing, the seasonal total is made by summing all nonmissing snow depths. These seasonal totals were then divided by the number of nonmissing days during each snow season (which is 195 if no data are missing), giving an average daily snow depth for each nonmissing season. A simple linear regression was fitted to the nonmissing yearly average daily depths, yielding a slope of 0.426 cm per century when all breakpoints are ignored and -1.548 cm per century when the five significant breakpoint are taken into account. Observe that the sign of these estimates agree with the ones fitted in our above computations.

[35] Some model validation diagnostics were performed. First, parameters for the seasonal model were estimated from the first 93 years of data only. This model does not contain a seasonal trend and only includes the five breakpoints deemed significant in the above analyses. A simulation was then conducted to estimate the time-varying mean (the unconditional mean) of this fitted model. This estimated mean is plotted against the last 10 years of snow depths in Figure 8. Except for 1997, the fitted model seems to describe this 10 years of data well. Notice that the fitted model has a slightly negative trend estimate. Because a breakpoint occurred in October 1992, the mean shift used for this breakpoint was taken as that estimated from all 103 years of data.

[36] Second, a set of residuals was computed for the daily model with a periodic trend and five breakpoints. These residuals, which are simply the difference between the observations and the 1-day-ahead predictions scaled by a daily standard deviation, are analyzed in Figure 9. The residuals appear to be symmetric about a zero mean (as seen in Figure 9, middle). The standard normal quantile plot in Figure 9 (top) shows that the residuals have some non-Gaussian features, but Gaussianity is not a requirement of residuals from a time series analysis. No 1-day-ahead residual exceeds 10 in magnitude, nor as Figure 9 (bottom) shows, does there appear to be significant lag one autocorrelation. This said, Figure 9 suggests that the model could be improved. Elaborating, large snowstorms frequently induce large positive residuals, especially when they occur at times when snow is typically not on the ground. Years where missing data is prevalent during midwinter (such as 1991) have very small residuals. Residuals during years with minimal snow tend to be small and negative. While incorporating a shot-type component into the model (i.e., a component that allows for rapid inputs of large amounts of snow) might remedy some of these aspects, this would be a difficult extension of this work.

6. Comments

[37] As in temperature trend analyses, breakpoints appear to be the most critical aspect to account for in estimating trends. With the Napoleon data, the sign of the trend estimate changes when breakpoints are ignored. In temperature studies, the effects of breakpoints are frequently illuminated by making reference series comparisons [*Menne and Williams*, 2005]. Such a tactic is not possible here as reference series are not readily available: it is questionable if

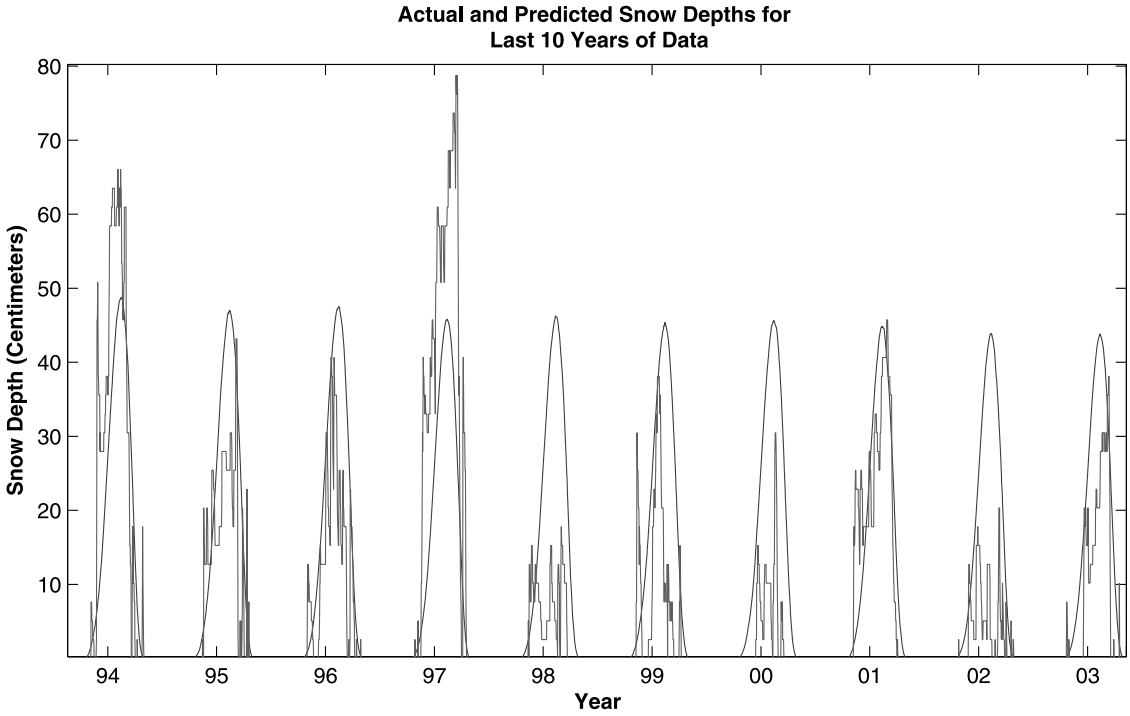

Figure 8. Predictions of last 10 years of data (smooth curve) against observed values (jagged curve). Note the slightly decreasing trend.

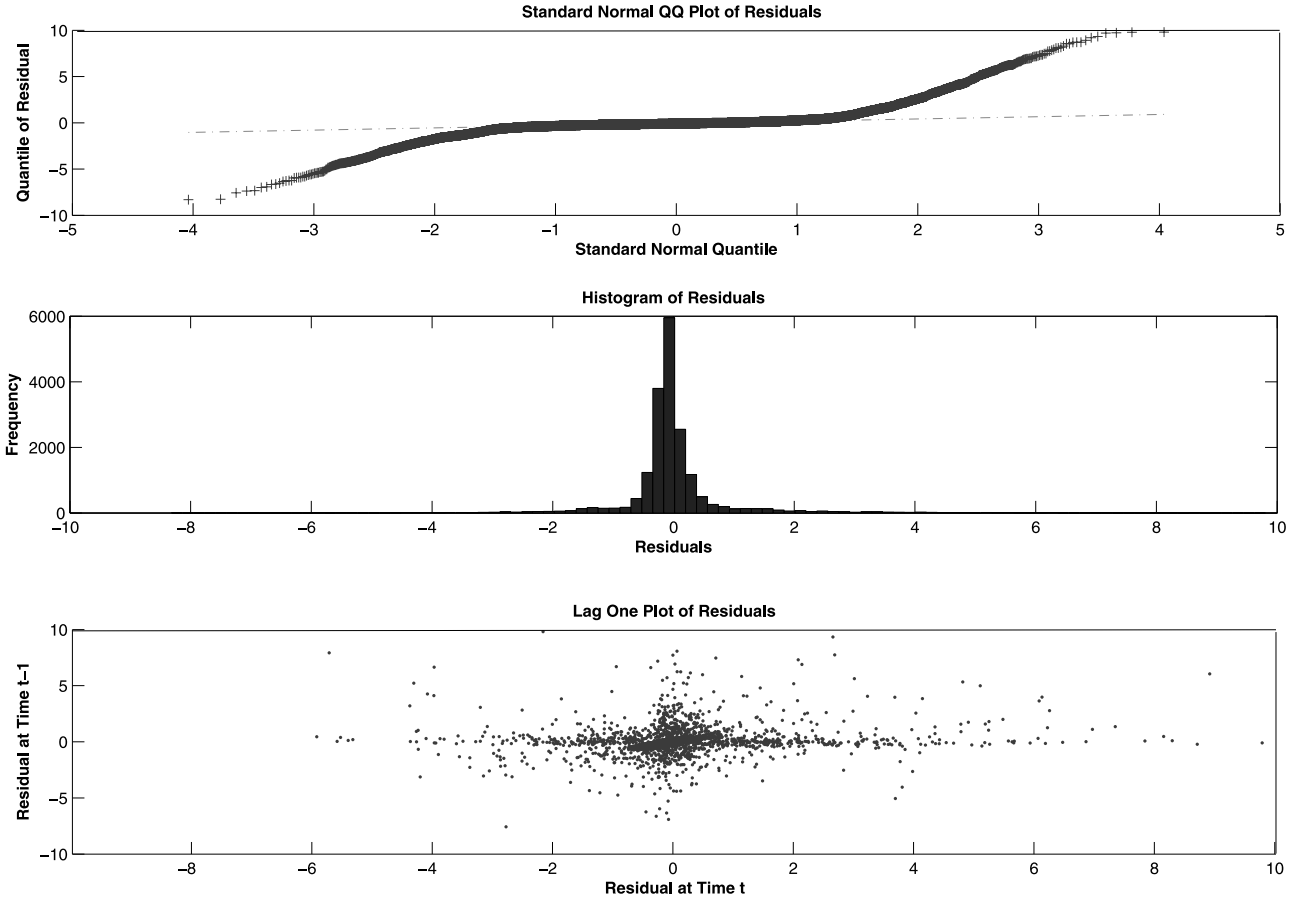

Figure 9. Diagnostic plots of model residuals. (top) QQ plot, (middle) histogram, and (bottom) lag one scatterplot.

any suitable reference station exists for Napoleon over its entire record. As snow depths can vary considerably over short geographical distances, reference station comparisons for snow data may also be more untrustworthy than those for temperature data. Also, the trend at any one station should be loosely interpreted. Ideally, trend estimates at many stations would be computed and spatially aggregated to make firm conclusions about changes in a geographic area. Such an endeavor requires a spatial analysis of trends from many stations, each of which could be computed as in this article. Modeling improvements might be possible if an accompanying temperature record (or other covariates) were available. Finally, true snow depth changes are likely to be nonlinear in time; of course, linear trends, regardless of the true trend structure, can always be interpreted as an average rate of change over the record.

Appendix A

[38] Appendix A derives the formula in (6). Using that Z_{t+1} is normally distributed with mean m_{t+1} and variance w_{t+1}^2, we have

$$E[X_{t+1}|X_t] = \int_{-X_t}^{\infty} (X_t + r) \frac{\exp\left\{-\frac{1}{2}\left(\frac{r - m_{t+1}}{w_{t+1}}\right)^2\right\}}{w_{t+1}\sqrt{2\pi}} dr$$

Making the substitution $u = (r - m_{t+1})/w_{t+1}$ gives

$$E[X_{t+1}|X_t] = \int_{-\kappa}^{\infty} [X_t + w_{t+1}u + m_{t+1}] \frac{e^{-u^2/2}}{\sqrt{2\pi}} du,$$

where $\kappa = (X_t + m_{t+1})/w_{t+1}$. Simplifying this gives

$$E[X_{t+1}|X_t] = (X_t + m_{t+1}) \int_{-\kappa}^{\infty} \frac{e^{-u^2/2}}{\sqrt{2\pi}} du + w_{t+1} \int_{-\kappa}^{\infty} \frac{u e^{-u^2/2}}{\sqrt{2\pi}} du.$$

Applying antiderivative properties of the standard normal distribution gives

$$E[X_{t+1}|X_t] = (X_t + m_{t+1})(1 - \Phi(-\kappa)) + w_{t+1}\phi(-\kappa),$$

which is (6) after symmetry of ϕ about zero is used.

References

Anderson, D. R., D. J. Sweeney, and T. A. Williams (1994), *Introduction to Statistics. Concepts and Applications*, 3rd ed., West, St. Paul, Minn.

Barnett, T. P., J. C. Adam, and P. Lettenmaier (2005), Potential impacts of a warming climate on water availability in snow-dominated regions, *Nature*, *438*, 303–309.

Barry, R. G. (1990), Evidence of recent changes in global snow and ice cover, *GeoJournal*, *20*, 121–127.

Basawa, I. V., and B. L. S. P. Rao (1980), *Statistical Inference for Stochastic Processes*, Academic, New York.

Blöschl, G. (1999), Scaling issues in snow hydrology, *Hydrol. Processes*, *13*, 2149–2175.

Boer, G. J., N. McFarlane, and M. Lazare (1992), Greenhouse gas-induced climate change simulated with the CCC second-generation general circulation model, *J. Clim.*, *5*, 1045–1077.

Brown, R. D., M. Hughes, and D. Robinson (1995), Characterizing the long term variability of snow cover extent over the interior of North America, *Ann. Glaciol.*, *21*, 45–50.

Burn, D. H. (1994), Hydrologic effects of climatic change in west-central Canada, *J. Hydrol.*, *160*, 53–70.

Cox, D. A., and H. D. Miller (1965), *The Theory of Stochastic Processes*, Chapman and Hall, London.

Fuller, W. A. (1996), *Introduction to Statistical Time Series*, 2nd ed., John Wiley, New York.

Grundstein, A., P. Todhunter, and T. L. Mote (2005), Snowpack control over the thermal offset of air and soil temperatures in eastern North Dakota, *Geophys. Res. Lett.*, *32*, L08503, doi:10.1029/2005GL022532.

Hamlet, A. F., P. W. Mote, M. P. Clark, and D. P. Lettenmaier (2005), Effects of temperature and precipitation variability on snowpack trends in the western United States, *J. Clim.*, *18*, 4545–4561.

Klimko, L. A., and P. I. Nelson (1978), On conditional least squares estimation for stochastic processes, *Ann. Stat.*, *6*, 629–642.

Kukla, G. J. (1979), Climatic role of snow covers, in *Sea Level, Ice and Climatic Change*, *IAHS Publ.*, *131*, 79–107.

Lu, Q., and R. B. Lund (2007), Simple linear regression with multiple changepoints, *Can. J. Stat.*, *37*, 447–458.

Marsh, P. (1999), Snowcover formation and melt: Recent advances and future prospects, *Hydrol. Processes*, *13*, 2117–2134.

Menne, M. J., and C. J. Williams Jr. (2005), Detection of undocumented changepoints using multiple test statistics and composite reference series, *J. Clim.*, *18*, 4271–4286.

Mote, P. W., A. F. Hamlet, M. P. Clark, and D. P. Lettenmaier (2005), Declining mountain snowpack in western North America, *Bull. Am. Meteorol. Soc.*, *86*, 39–49.

Myeni, R. B., C. D. Keeling, C. J. Tucker, G. Asrar, and R. R. Nemani (1997), Increased plant growth in the northern high latitudes from 1981 to 1991, *Nature*, *386*, 698–702.

Perona, P. A., A. Porporato, and L. Ridolfi (2007), A stochastic process for the interannual snow storage and melting dynamics, *J. Geophys. Res.*, *112*, D08107, doi:10.1029/2006JD007798.

Robinson, D. A. (1993), Historical daily climatic data for the United States, paper presented at Eighth Conference on Applied Climatology, Am. Meteorol. Soc., Anaheim, Calif.

Schmidt, W. L., W. D. Gosnold, and J. W. Enz (2001), A decade of air-ground temperature exchange from Fargo, ND, *Global Planet. Change*, *29*, 311–325.

A. J. Grundstein and T. L. Mote, Department of Geography, University of Georgia, Athens, GA 30602, USA.

R. Lund and J. Woody, Department of Mathematical Sciences, Clemson University, Clemson, SC 29634-0975, USA. (lund@clemson.edu)